## 1. INTRODUCTION

Since the late 90s, fibre reinforced SiC ceramic matrix composites (CMCs) have been considered for nuclear reactor components, such as first walls and blankets [1,2,3]. These components are subjected to temperatures typically ranging from 600 to 1000℃, and to stresses from 60 to 150 MPa, the lower values being associated with the higher temperatures and vice-versa [1]. In these conditions, ceramic materials offer promising characteristics, in terms of mechanical performances, chemical stability and radiation resistance. Fibre reinforced ceramic matrix composites are most often considered, because their fracture toughness and thermal shock/thermal fatigue resistance are higher than those of the correspondent monolithic materials. Moreover, their properties can be tailored to fit a specific application, by choosing fibres, matrix, fibre/matrix interface and processing route [4]. In particular, the characteristics of the fibre/matrix interface has proven of paramount importance in determining the mechanical behaviour, influencing the stress distribution, the extent of pullout and of crack bridging [5]. SiC based materials are particularly interesting because of their radiation resistance [1,2].

Composite materials typically show a rather 'ductile' behaviour: even when the matrix cracks and the stress-strain curve deviates from linearity, the fibre are still able to sustain load and the loss of mechanical properties is gradual. The failure strain is remarkable and the high dissipated energy is related to elevated toughness, that can reach values above 25 $MPa \cdot m^{0.5}$, independent of temperature, up to fibre stability [6].

Creep failure has been observed in CMCs, including $SiC_f/SiC$ [7,8,9,10]. The creep behaviour of CMCs usually depends on the ratio between the fibre creep rate and the matrix creep rate. In most cases the fibre creep rate is greater, and matrix microcracking and fibre bridging control the material damage and behaviour [11,12]. These considerations presume that the fibre/matrix interface is weak enough to allow fibre and matrix to deform and break independently, to some extent [4].

CMCs components in fusion reactors are not usually subject to fatiguing stresses, but occasional thermal cycles and reactor "off normal" events may result in a cyclical mechanical loading. For this reason, the fatigue behaviour of the material has an applicative interest and was extensively investigated. When subject to a cyclical loading, both at RT and at HT, $SiC_f/SiC$ composites usually show a definite fatigue limit, with the stress-strain curves forming hysteresis loops and with a progressive decrease of Young's modulus, in connection with the presence of mechanisms that progressively degrade the mechanical performance of the material, such as change in the fibre/matrix interface, fibre degradation due to wear, matrix microcracking and subcritical crack propagation, [13,14,15] . Authors have measured a fatigue limit of about 80% of ultimate tensile strength, UTS, at room temperature [12] while according to other works [7] the fatigue limit of CMCs is more strictly connected to the stress level at which nonlinear behaviour begins, $\sigma_{pl}$ than to UTS.

At high temperature, the fatigue mechanisms are still active and may even be enhanced by chemical interaction with the atmosphere, if, for instance, the fibres are carbon coated and the atmosphere is oxidizing. If the temperature is high enough to allow fibre and/or matrix creep to take place, the creep mechanisms interfere with cyclical damage, resulting in a reduction of time to failure [4,12].

The goal of this experimental work was to determine if the commercial-grade material is mechanically suitable for the described nuclear application, in particular for what concerns resistance, cyclical fatigue and creep properties. At the same time, the microstructure and fracture mechanisms were studied, in order to understand what micro-scale phenomena control the material failure at different temperatures and in different loading conditions (monotonic, cyclical and constant-stress loading).

## 2. MATERIAL CHARACTERISTICS

The composite is made of Tyranno SA3 fibres (UBE Industries-J) up to a fibre volume percentage of about 40%. The preforms were obtained by stacking and pressing plain weave cloths up to a thickness of about 3 mm. The preforms were subjected to a short isothermal CVI run to grow a thin debonding carbon interphase (about 80 nm) and afterwards were infiltrated by isothermal-CVI. Finally they underwent a CVD process to grow a SiC coating about 80 μm thick. All the densification processes were carried out with no clamping of the fibre performs. The final mean thickness of the composites is about 3.7 mm. The apparent density is 2.70 $g/cm^3$; the total porosity, about 13%, is mainly located in large zones between layers. The single clothes appear, in general, well bonded and coated by the SiC matrix. The material was furnished for testing in plates 200 x 200 $mm^2$.

## 3. EXPERIMENTAL PROCEDURE

### 3.1 Specimens preparation

Specimens for monotonic and fatigue tests were cut according to the European standard EN 658-1, except for the thickness, which was not reduced to the standard value in order to leave the outer fibre layers and coating unaltered.

Reduced-size specimens (4 x 45 x thickness) were prepared for the creep tests. Additional small specimens were cut for monotonic tests, in order to have a comparison with the standard specimens.

### 3.2 Mechanical testing

Monotonic flexural tests were made at room temperature, at 600°C and at 1000°C using a servohydraulic machine (MTS 880). The tests were conducted according to the European standard (EN 658-1) on 2 specimens for each temperature.

Monotonic tests at high temperature (2 tests at 600°C and 2 at 1000 °C) were made on reduced size specimens, in order to have a reference value for the creep test.

Creep behaviour was evaluated by 4-point-bending stress rupture tests, performed on the specimen of reduced size. Creep runout was arbitrarily defined at 1000 hours.

Cyclic fatigue tests were made at room temperature, at 600°C and at 1000°C. Bending tests were made using a sinusoidal wave form stress amplitude and a frequency of 2 Hz. The peak stress ranged between a significant and a small fraction of the monotonic flexural strength. A small load (50 N), corresponding to a minimum stress of about 30 MPa, was imposed in order to keep the specimen in place in the bending fixture. The test duration was limited to $0.8 \times 10^5$ cycles at room temperature and $0.5 \times 10^5$ at elevated temperature.

All the tests at high temperature were conducted with circulating inert gas (Argon), but the oxygen content was not monitored.

## 4. RESULTS AND DISCUSSION

### 4.1 Monotonic tests

The flexural resistance of the material is in good agreement with that of similar CMCs [4,16]. The resistance decreases with increasing temperature: the values ranges are 327 - 410 MPa at RT, 295 - 310 MPa at 600°C and 249 - 287 at 1000°C. The decrease of Young's modulus is less evident: the values pass from 226 - 250 GPa at RT to 212 – 254 GPa at 600°C, and 181 - 212 GPa at 1000°C.

The failure mode is typical of ceramic composites in bending: a crack propagates through the layers, due to the tensile stresses and only in a secondary stage bifurcates and deflects drastically, assuming a direction parallel to the specimen's faces, showing that the delaminations do not affect the materials behaviour in the first stage of failure. Fig. 1 shows typical stress-strain curves at different temperatures, the main features are the decrease of the tangent modulus after an initial linear region and the limited strain to failure. The stress at which curves deviate from linearity, $\sigma_{pl}$, is about 96 MPa, both at RT and at 600°C, but decreases to about 81 MPa at 1000°C.

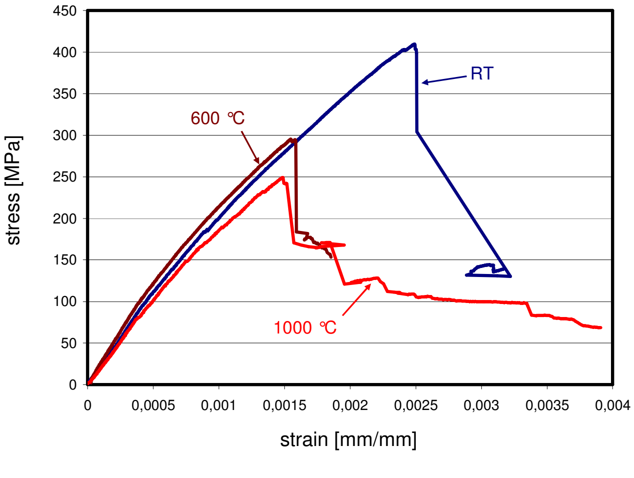


Fig. 1 - stress-strain curves at different test temperatures. The curves deviate from linearity at 70-100 MPa and subsequently the tangent modulus decreases with increasing load, indicating probable matrix cracking.

The strain to failure is limited. This seem to indicate that the fibre/matrix debonding and pullout is very limited, so that unbroken fibres can transfer load to the matrix, producing a smaller crack spacing [11]. SEM observations of fracture surfaces (Fig. 2) show that although the pull out length appears limited, in all tests, the specimens fractured at RT show a slightly larger pull-out, compared to those fractured at 1000℃. A limited decohesion of the fibre/matrix interphase was observed in both cases. This behaviour can be attributed to the limited thickness of the carbon interphase and the external roughness of the fibres.

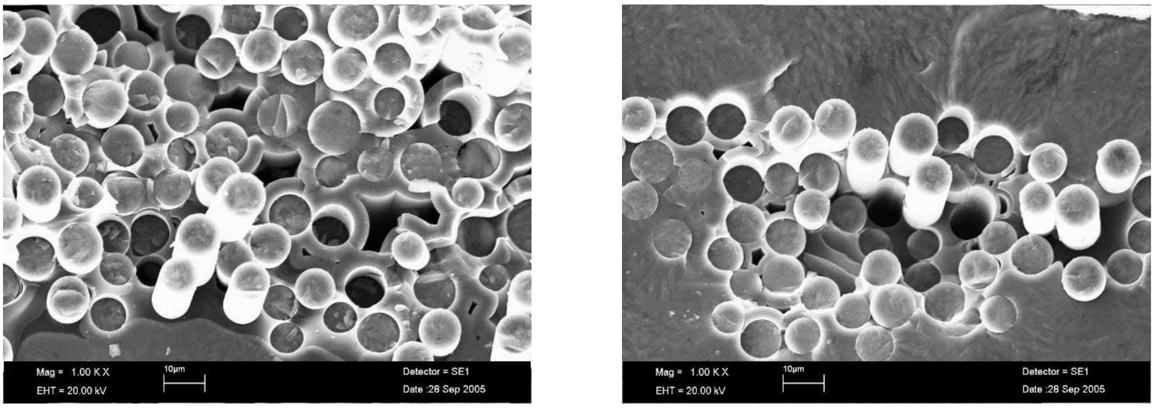


Fig. 2 - fracture surfaces of specimens tested at RT (left) and at 1000℃ (right) showing a limited pullout.

**4.2 Creep tests (stress rupture tests)**

At 600℃ the material seems to be slightly sensitive to creep damage: the specimens tested at a high maximum stress (close or higher than the MOR) break in very short time, while at 200 MPa or less, the specimens sustain the load without detectable damage, for at least 1000 hours. At 1000℃, the time to rupture decreases with increasing applied stress; only at stresses not higher than 60 MPa the runout time is reached without evident damage in the specimen.

The time-to-failure values and creep rates, calculated in the secondary stage, are represented in the graph of Fig. 3 and

Fig. 4. They are in agreement with literature data [4,17] and fit power laws of the type $t = A\sigma^{1/n}$ $d\varepsilon/dt = B\,\sigma^m$ respectively.

With the exception of the specimens broken in very rapid times, the specimens break in the secondary stage of creep (stationary stage), when the creep rate is constant. A tertiary stage has not been observed in our tests. The fracture is brittle, the specimens break apart completely with very low strains. SEM observation of the fracture surface shows that, even to a limited extent, time-dependent and energy dissipative mechanisms, such as pullout and damage of the fibre-matrix interface are present (see

Fig. 5).

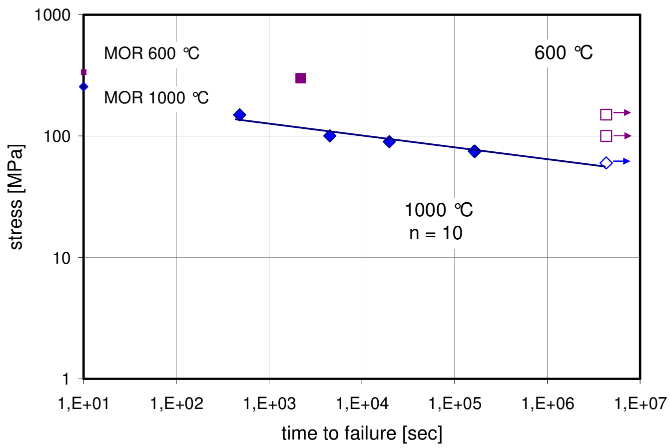


Fig. 3 - creep data at 600 ℃ and 1000 ℃. The material seems to be slightly sensitive to creep damage at 600℃, while at 1000℃ the time to rupture decreases with increasing stress.

Since the interfacial shear strength of the composites is very high, due to fibre roughness and interphase thickness, the sliding of the bridging fibre is modest. At high loads, the extensive matrix cracking induces fibres creep. The fibres break in short time and the progressive matrix reloading is high enough to determine full matrix cracking and specimen failure. At low loads, the lifetime increases significantly. In this case the matrix cracking is limited and during the consequent creep of the fibres bridging the cracks, the time-dependent redistribution of stress from fibres to matrix determine the matrix crack opening and the loading of additional undamaged fibres. In these conditions, due to the further fibre creep, the fibres start to break at stress concentration sites. Only when the fibre rupture reaches a critical level, the heavy reloading of the matrix leads to the final fracture of the specimen.

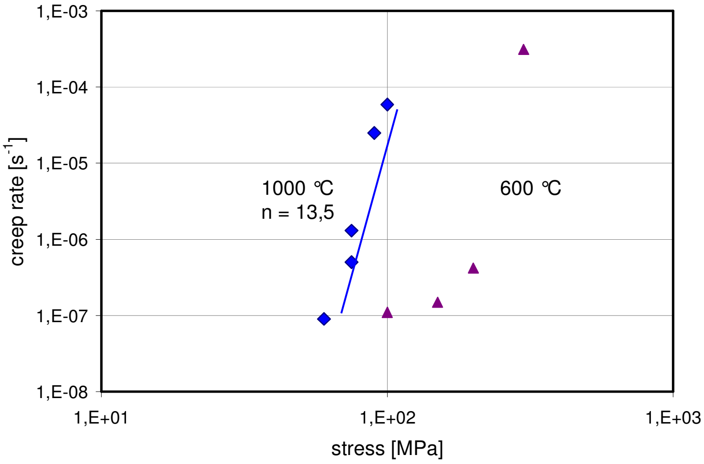


Fig. 4 – creep rate, calculated in the secondary stage, plotted as a function of the applied stress. The data at 1000°C fit a power law.

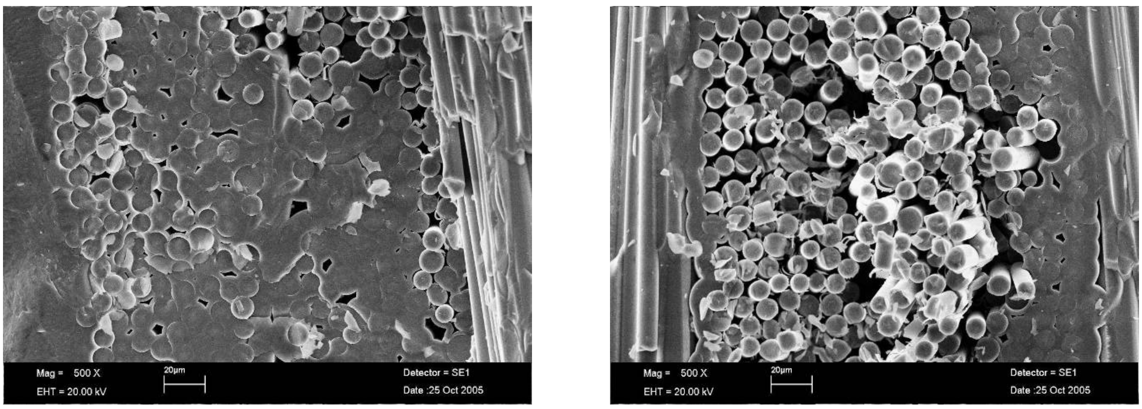

Fig. 5 - details of the fracture surface of specimen tested at 1000°C.
Left: specimen tested at 90 MPa. Right: specimen tested at 75 MPa.
Although very low, the pullout is higher at low load

**4.3 Fatigue tests**

The results at RT show that the material has a good fatigue behaviour: no failure occurs after $0.8 \times 10^5$ cycles at a peak load up to 98 % of the flexural strength, a value well above the matrix cracking stress $\sigma_{pl}$. This result is consistent with literature data [4,14] and indicates that the composite can avoid the matrix crack propagation produced in the first loading cycle, in fact the microcracking process is arrested during cyclic loading and remains stationary because the fibre bridging in the crack wake reduce stress intensity at the crack tip.

The RT stress-strain loops, which are present even at peak loads well below $\sigma_{pl}$, indicate that active fatigue mechanisms (effective fibre-interface sliding) dissipate energy (thus the loops) but do not damage the material, since, with increasing cycle number, the tangential elastic modulus remains and the loop area remain almost unchanged.

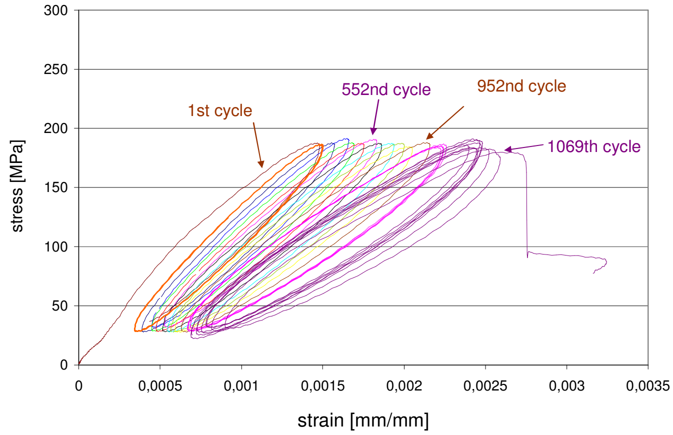


Fig. 6 - stress strain loops during a cyclical test at 1000℃; the curves show an evident progressive damage due to the cyclical loading: the tangent modulus decreases and there is an evident strain ratchetting.

At high temperature, the material behaviour is different. Stress-strain loops (Fig. 6) are evidenced, but the elastic modulus gradually decreases (see Fig. 7). This phenomenon is related to progressive material damage [10,15], such as degradation of the fibre-matrix interphase. The damage is indicated also by the increase of the loop area and by the strain ratchetting (the hysteresis loops shift to the right of the strain axis, with increasing cycle number) [7]. As it is shown in the graph of Fig. 8, where the peak stress is plotted as a function of fatigue life (Wöhler curve), the fatigue limit $\sigma_f$ is about 70% of MOR at 600℃ (212 MPa, $\sigma_f > \sigma_{pl}$) and 30 % of MOR at 1000℃ (67 MPa, $\sigma_f < \sigma_{pl}$).

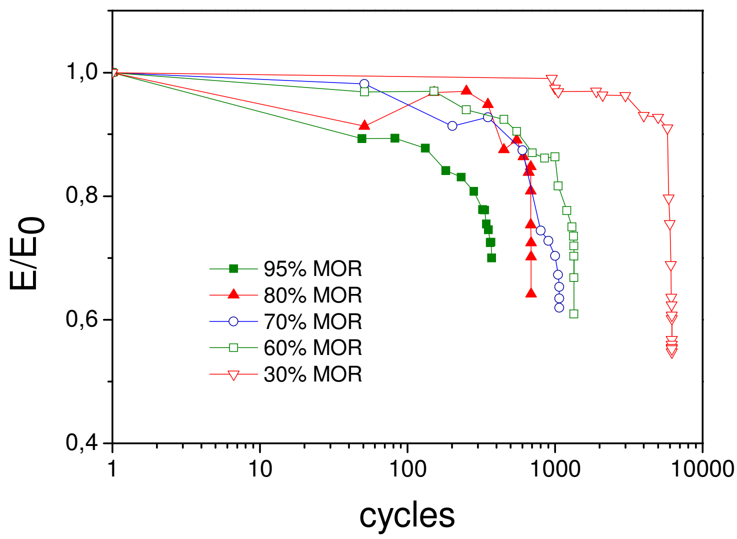


Fig. 7 – variation of tangent modulus during a cyclical tests at 1000℃ at various peak stresses

Fig. 9 shows the fracture surface of a fatigue specimen tested at 1000℃ at a peak load of 40% MOR. The pullout is very limited.
Creep damage seems to influence the fatigue behaviour. The reduction of the tangent modulus and the strain ratchetting can be related to creep damage, as it has been found by several authors [4,12]. It is also interesting to point out that, when the peak load is lower than the material creep limit, the specimens sustain the fatigue load for at least 1000 hours (test runout). In such cases the strain ratchetting is of the same order of magnitude of the creep strain measured with similar stresses.
Even if the fatigue performances at high temperature decrease, the material appears a suitable fusion reactor structural material, since very low cycle fatigue is expected for this application and the material exhibits a fatigue limit.

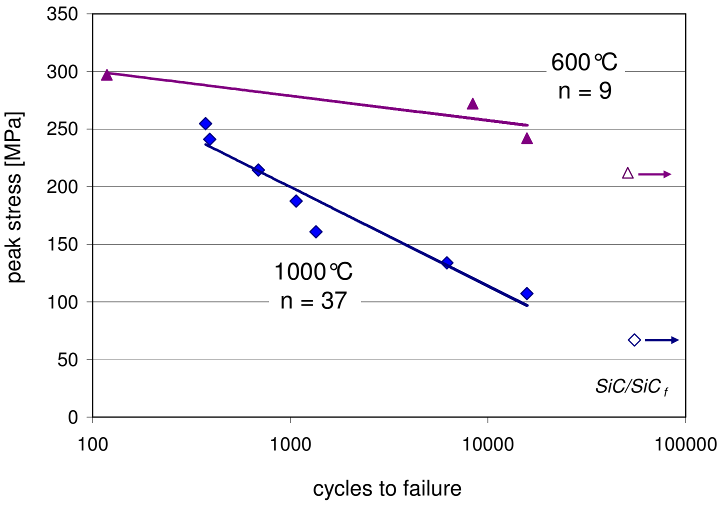


Fig. 8 - Wöhler curves at 600°C and 1000°C; the material seems to be more fatigue sensitive at 1000 °C than at 600 °C. At both temperatures a peak stress has been identified at which the material does not show fatigue damage after at least $0.5 \cdot 10^5$ cycles.
Open symbols indicate interrupted tests.

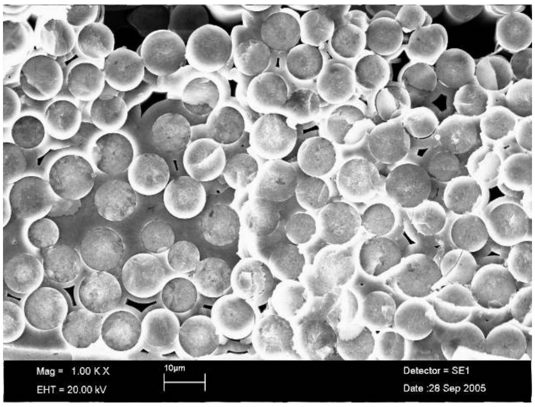


Fig. 9 - SEM image of the fracture surface of a fatigue specimen tested at 1000°C at a peak load of 40% MOR. The pullout is nearly absent.

## 5. CONCLUSIONS

The mechanical behaviour of commercial grade 2D-$SiC_f$/SiC composites has been evaluated. The mechanical performances satisfy the specification for the material procurement and the material can be assumed for fusion reactor studies. the data are in good agreement with literature data obtained on similar materials.

In the monotonic tests the material showed a limited elongation and degradation of properties at high temperature. Creep behaviour was studied by means of stress rupture flexural tests. The material showed a low sensitivity to creep damage at 600°C, while at 1000°C the specimens crept according to a power law. Flexural fatigue behaviour was investigated by means of 4-point bending tests; the material showed excellent results at RT, but the fatigue resistance decreases with increasing temperature. This can be related to the onset of creep mechanisms.

The results indicate that further R&D on fibre-matrix interphase and on the time-dependent damage mechanisms is necessary to improve the mechanical behaviour of the material.


## ACKNOWLEDGEMENTS

The author wishes to warmly thank Dr. B. Riccardi of ENEA, CR Frascati and Dr. M. Labanti of ENEA, CR Faenza for their precious suggestions. She also thanks Mr Martignani, Mr Pilotti and Mr Ricci of ENEA, CR Faenza for the support with creep tests and microscopical analysis.

**REFERENCES**


[1] R.H. Jones, D. Steiner, H.L. Heinish, G.A. Newsome and H.M. Kerch: J. Nucl. Mater. Vol. 245 (1997), pp. 87-107 (journal)

[2] R.H. Jones, L. Giancarli, A. Hasegawa, Y. Katoh, A. Kohyama, B. Riccardi, L.L. Snead and W.J. Weber: J. Nucl. Mat. Vol. 307-311 (2002), pp. 1057-1072 (journal)

[3] R. Raffray, R.H. Jones, G. Aiello, M. Billone, L. Giancarli, H. Golfier, A. Hasegawa, Y. Katoh, A. Kohyama, B. Riccardi, and M.S. Tillack, Fusion Eng. Des., Vol. 55, (2001) pp. 55-95 (journal)

[4] S. Zhu, M. Mizuno, Y. Kagawa and Y. Mutoh: Comp. Sci. Tech., Vol. 59 (1999) pp 833-851 (journal)

[5] Y.-C. Chiang: Comp. Sci. Tech. Vol. 61 (2001) 1743-1756 (journal)

[6] R.H. Jones and C. H. Henager Jr: J. Eur. Ceram. Soc, Vol. 25 (2005) 1717-1722 (journal)

[7] J.W. Holmes: J. Am. Ceram. Soc., Vol 74 (1991) pp.1639-1645 (journal)

[8] A.G. Evans, F.W. Zok and R.M. McMeeking: Acta Metall. Mater. Vol. 43 (1995) pp. 859-875 (journal)

[9] C.A. Lewinsohn, R.H. Jones, G.E. Youngblood and C.H. Henager Jr: J. Nucl. Mat. Vol. 258-263 (1998) pp. 1557-1561 (journal)

[10] J.L. Chermant, G. Boitier, S. Darzens, G. Farizy, J. Vicens and J.C. Sangleboeuf: J. Eur. Ceram. Soc. Vol. 22 (2002) pp. 2443-2460 (journal)

[11] F. Lamouroux, J.L. Vallés and M. Steen: Comp. Eng. Vol 5 (1995) pp. 1379-1386 (journal)

[12] S. Zhu, M. Mizuno, Y. Kagawa, J. Cao, Y. Nagano and H. Kaya: Mat. Sci. Eng. A Vol. 225 (1997), pp. 69-77 (journal)

[13] A.G. Evans and C. Weber: Mat. Sci. Eng, Vol. A208 (1996) pp. 1-6 (journal)

[14] S.J. Zhu, Y. Kagawa, M. Mizuno, S.Q. Guo, Y. Nagano and H. Kaya: Mat. Sci. Eng. A Vol. 220 (1996), pp. 100-108 (journal)

[15] Y. Miyashita, K. Kanda, S. Zhu, Y. Mutoh, M. Mizuno and A.J. McEvily: Int. J. Fat. Vol. 24 (2002), pp. 241-248 (journal)

[16] B. Riccardi, M. Labanti, E. Trentini, S. Roccella and E. Visca: Proceedings of the "6th IEA Workshop on SiCf/SiC", Boston 2004 (book)

[17] S.R. Choi and J.P. Gyekenyesi: Int. J. Fat. Vol 27 (2005) pp. 503-510 (journal)